Ultraviolet Absorbance and Circular Dichroism of Pf1 Virus: Nucleotide/Subunit Ratio of Unity, Hyperchromic Tyrosines and DNA Bases, and High Helicity in the Subunits[†,‡]

Leondios G. Kostrikis,[§] David J. Liu, and Loren A. Day[*]

The Public Health Research Institute, 455 First Avenue, New York, New York 10016

Received August 2, 1993; Revised Manuscript Received November 30, 1993[⊗]

ABSTRACT: Data have been obtained for the Pf1 virion that establish its stoichiometry and conformational features of its DNA and its protein. The absorbance spectrum of the dissociated virus under alkaline denaturing conditions is fit exactly by spectra for DNA and protein at a mole ratio of one nucleotide per protein subunit. This result, together with three previous values by independent methods, establishes that the nucleotide/subunit ratio (n/s) of Pf1 is unity. The absorbance spectrum of DNA in the intact native virus is assigned as the spectrum for heat denatured Pf1 DNA, with $\epsilon(P) = 8400\ M^{-1}\ cm^{-1}$ at 259 nm. The absorbance spectrum assigned to protein (two tyrosines) in the intact virus has $\langle\epsilon(Y)\rangle = 2500\ M^{-1}\ cm^{-1}$ per tyrosine at λ_{max} of 281.5 nm; this is the most red-shifted and hyperchromic tyrosine spectrum known. The CD spectrum of the intact virus from 250 to 320 nm has no apparent DNA contribution, but has a strong contribution from the red-shifted tyrosine(s). The CD spectrum from 185 to 250 nm has the shape of α-helical CD reference spectra, but is perceptibly blue-shifted, with a crossover from negative to positive ellipticity at 199.7 nm, and it has very high amplitudes (e.g. $[\theta_{207.5nm}] = -44\ 000$ deg cm^2 dmol^{-1}). This spectrum indicates completely helical protein in the virus, with a predominance of α-helix and perhaps some 3_{10}-helix. The unit n/s ratio, the high absorbance and negligible near-UV CD for the DNA bases, and the high amplitudes for the helical protein are critical input data for the determination of Pf1 virus structure.

Pf1 virus, which infects *Pseudomonas aeruginosa* strain K, is the longest of all known filamentous viruses (Takeya & Amako, 1966; Bradley, 1973). An electron micrograph of a single virion, displaying its extreme length (2000 nm) and small diameter (less than 7 nm), is shown in Figure 1, together with a diagram of the relation of the DNA and protein. The topologically circular single-stranded genome of 7349 nucleotides (Hill *et al.*, 1991) extends from one end of the virion to the other and back again, forming two antiparallel strands along the contour, with fold-backs at the ends. About 94% of the mass of the virion is protein, with 1% from minor components and 99% from the major coat protein of 46 amino acids. X-ray fiber diffraction has shown the major coat protein subunits in the virion to be arranged in a helical array, with approximately 5.4 subunits per turn of a one-start helix of 15- to 16-Å pitch (Marvin *et al.*, 1974; Wiseman & Day, 1977; Makowski & Caspar, 1981; Marzec & Day, 1988). There are two aromatic chromophores, tyrosine-25 (Y_{25}) and tyrosine-40 (Y_{40}). Y_{40} is near the DNA and Y_{25} is near the surface of the virus (Nave *et al.*, 1981; Nambudripad *et al.*, 1991a). Y_{25} has a pK_a of 11.4 and appears to be more fluorescent than free tyrosine, whereas Y_{40} cannot be titrated in intact virus and has essentially no fluorescence (Day & Wiseman, 1978; Day *et al.*, 1979; Greulich & Wijnaendts Van Resandt, 1984). Y_{25} is accessible to enzyme-catalyzed iodination but Y_{40} is not (Nave *et al.*, 1981). Both tyrosines appear to be H-bond acceptors and donors according to Raman spectroscopy (Thomas & Murphy, 1975; Thomas *et al.*, 1983) and also to analyses of UV absorbance derivative spectra (Kostrikis, 1993; and see below). Two detailed models of the

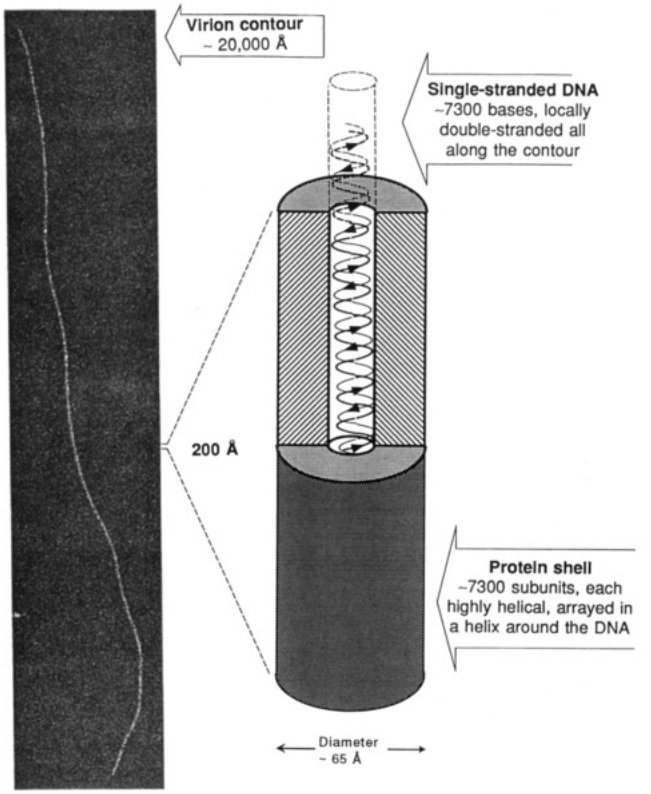

FIGURE 1: (Left) Scanning transmission electron micrograph of an unstained Pf1 virion from Kostrikis *et al.* (1991); (right) schematic representation of an axial slab 200 Å long. The amino acid sequence of the coat protein subunit is GVIDTSAVESAITDGQGDMKAIGGYIVGALVILAVAGLIYSMLRKA.

[†] Principal financial support was through NIH grant GM42286 awarded to L.A.D. D.J.L. was supported in part by the Sackler Institute for Graduate Studies, New York University School of Medicine.

[‡] From part of the Ph.D. thesis of L.G.K. in the Department of Chemistry, New York University.

[*] To whom correspondence should be addressed.

[§] Present address: Aaron Diamond AIDS Research Center, 455 First Avenue, New York, N.Y. 10016

[⊗] Abstract published in *Advance ACS Abstracts,* February 1, 1994.

0006-2960/94/0433-1694$04.50/0

protein subunit structure have been proposed, one having all 46 residues in a gently curving α-helix (Marvin *et al.*, 1987, 1992) and the other having a loop of seven amino acid residues not in an α-helix (Nambudripad *et al.*, 1991a,b).

From the virion length and the number of nucleotides, it has been known for a long time that the DNA conformation is highly extended (Wiseman & Day, 1977; Day & Wiseman, 1978; Day *et al.*, 1988a). The location of the DNA at the center of the structure has been deduced from radial density distributions (Makowski & Caspar, 1978; Reisberg, 1989), and some of its structural parameters have been obtained from chemical and spectroscopic data. The ratio of nucleotides per protein subunit (n/s) is one of the key parameters. It gives the overall chemical stoichiometry and constrains the ways the nucleic acid and protein helices can be interconnected, as discussed in detail by Marzec and Day (1983). Measured values of n/s for Pf1 have ranged from 0.9 to 1.1, depending on the sample and the method used (Wiseman *et al.*, 1976; Wiseman & Day, 1977; Reisberg, 1989; Kostrikis *et al.*, 1991; Kostrikis, 1993). On the basis of an assumed n/s of unity and other data then available, Day *et al.* (1979) proposed an everted DNA model in which the two antiparallel strands are wound in helices of about 15-Å pitch with phosphates very near the viral axis and unstacked bases directed outward. This type of model was developed further by Day *et al.* (1988a) on the basis of sugar pucker from Raman scattering (Thomas *et al.*, 1983, 1988), phosphate group orientation from NMR (Cross *et al.*, 1983), base accessibility from Ag(I) probing (Casadevall & Day, 1983; Day *et al.*, 1988b), and base plane orientation from linear dichroism (Clack & Gray, 1992). A very different DNA model, which has opposite-strand base–base stacking, was recently proposed by Marvin *et al.* (1992).

In this paper, we report a spectroscopic determination of Pf1 DNA–protein stoichiometry, as well as analyses of UV absorbance and CD spectra for the Pf1 virion and its isolated components. The data establish a unit n/s ratio, unique among filamentous phage and all nucleoproteins. In accord with structural implications of the unit ratio, the absorbance and CD data demonstrate a minimal level of base–base electronic spectral interactions. The far-UV CD data suggest the possible presence of some 3_{10}-helix in an otherwise highly, if not completely, α-helical protein subunit.

MATERIALS AND METHODS

Virus, DNA, and Protein. Pf1 virus and its host, *P. aeruginosa* (strain K), were originally obtained from K. Amako (Takeya & Amako, 1966). Pf1 virus was grown from a single plaque. Infected bacteria from the plaque were cultured in LB medium for 6 h or less. The virus was concentrated from the medium by poly(ethylene glycol) precipitation (Yamamoto *et al.*, 1970), then resuspended and subjected to two rounds of differential sedimentation, and two rounds of CsCl buoyant density equilibrium sedimentation. The CsCl-banded virus formed a visible bluish band at 1.286 g cm^{-3} (Kostrikis *et al.*, 1991). The central fraction of each band ($\sim^1/_3$) in each of the two successive runs was recovered. The virus recovered from the second gradient was dialyzed against several changes of distilled water. The final yield of purified virus (10–20 mg per liter of culture) was only about 5–10% of the total amount of virus produced by the infected cells.

The samples were characterized for yield, for titer, for amino acid sequence of the N-terminal region of the major coat protein, for DNA sequence of gene VIII (major coat protein gene), and for length homogeneity by electron microscopy. Final stock solutions of virus contained 5–10 $OD_{272.5nm}$/mL and had titers corresponding to about 35 plaque forming units per 100 physical particles. Concentrations were determined with a scatter-corrected absorbance coefficient for Pf1 virus of 2.12 mg^{-1} cm^2 at 272.5 nm in 10 mM sodium phosphate, pH 7.2 (see Results). This coefficient is based on the unit nucleotide per subunit ratio n/s (see Results), the molar extinction coefficients for separate DNA and protein, and the formula weights of the DNA and protein. The protein sequencing was performed on a PI 2090E Integrated Micro-Sequencing System with the intact virus as input material. Nineteen cycles showed the first 19 amino acids of the mature gene VIII protein, with no other signals detectable above background. No proteinaceous material other than that from Pf1 virus was detected by gels or by protein sequencing, and the DNA sequencing confirmed that the gene VIII was wild type. Pf1 purified in this way is homogeneous with respect to virion length, as revealed by STEM studies (Kostrikis *et al.*, 1991).

Pf1 ssDNA was isolated from the purified virus by extracting the protein with phenol. Approximately 1.5 mg of virus in 500 μL of 10 mM Tris-HCl and 0.1 mM EDTA buffer, pH 8.0, was extracted with three successive additions of 250 μL of buffer-saturated phenol. The DNA was precipitated from the aqueous phase and resuspended in the same buffer, with two repeat precipitations and resuspensions. Since the presence of traces of gene VIII protein (two tyrosines per protein) or phenol in DNA preparations could affect the spectroscopic determination of the n/s ratio, the UV absorption of each DNA solution was determined at high alkaline conditions (pH 13.3) and compared with the theoretical spectrum generated as the weighted sum of UV spectra at this pH of the 5′ monophosphate nucleotides (19.4% A, 31.3% C, 30.2% G, 19.1% T) (Hill *et al.*, 1991). At pH 13.3, the phenolate groups of the protein or phenolate itself were easily detected, and if present, the DNA solution was further purified.

Pf1 protein was recovered from the phenol phases according to a procedure used for fd protein (Knippers & Hoffmann-Berling, 1966). The three phenolic phases were pooled (750 μL) and extracted four times with equal volumes of 10 mM Tris-HCl and 0.1 mM EDTA. The phenolic layer containing the protein was diluted with two volumes of methanol, and the mixture was dialyzed successively against 50% methanol–water, 30% methanol–water, and then distilled water. The turbid protein suspension was freeze dried, and the protein was stored at 4 °C. Protein yield was about 90%.

Ultraviolet Absorbance Spectra, Derivative Absorbance Spectra, and Melting Curves. Ultraviolet (UV) absorbance spectra were recorded on a Cary 219 spectrophotometer interfaced to a PC (386SX20) computer for acquisition of data every 0.1 nm. The interface was built around an Intel 8255 PIO chip, and programs in TurboPascal and Turbo-Assembler (Borland International) were written to drive it. Wavelength accuracy was better than ±0.2 nm, according to calibrations with mercury vapor, and wavelength repeatability with within ±0.05 nm. Spectra were recorded at scan rates of 0.5–1.0 nm/s, at a period of 0.5 s, and at slit widths of 0.5–1.0 nm. Derivative spectra ($\Delta A/\Delta\lambda$ versus wavelength) were obtained numerically. It was ascertained that intervals of $\Delta\lambda$ = 1 nm yield reliable derivative spectra. As $\Delta\lambda$ was reduced to 0.1 nm, the spectra remained similar to each other, simply noisier, as expected.

Melting curves of Pf1 single-stranded DNA in 10 mM sodium phosphate, 1% SDS at DNA concentrations of 240

μM in nucleotides were measured at 259 nm in a 5-mm pathlength cell with a thermoelectrically controlled Perkin-Elmer 552 spectrophotometer interfaced to a PC-XT computer (Dept. of Chem., N.Y.U.). The heating rate was 1.0 °C/min from room temperature to 100 °C.

Determinations of (n/s). Small aliquots (6–10 μL) of purified Pf1 virus (2–4 mg mL^{-1}) were diluted and disrupted into 0.6–1.0 mL of *cracking buffer* (0.2 M NaOH, 1% SDS, and 8 M urea, pH 13.3), and absorbance spectra were recorded from 340 to 250 nm. Molar reference spectra for the isolated DNA and protein were obtained in the same buffer in the same way. Linear regressions performed on the spectra of the mixtures were for the sets of (~900) equations

$$A_{\lambda_i} = \epsilon_{\lambda_i \mathrm{DNA}}\,[\text{nucleotides}] + \epsilon_{\lambda_i \mathrm{protein}}\,[\text{subunits}]$$

where the A_{λ_i} are the observed absorbance values of the disrupted virus at the wavelengths λ_i, the $\epsilon_{\lambda_i \mathrm{DNA}}$ are the DNA molar extinction coefficients, the $\epsilon_{\lambda_i \mathrm{protein}}$ are the protein molar extinction coefficients (see results), and the bracketed quantities are the desired molar concentrations.

Circular Dichroism Measurements. Circular dichroism spectra were recorded on a Cary 60 spectropolarimeter with a CD attachment. The alignment and calibration of the CD module was carried out so that (1) for samples of camphorsulfonic acid d_{10} (CSA), ratios of the CD amplitude at 192.5 nm to that at 290.5 nm fell between 2.0 and 2.1; (2) samples of achiral chromophores (phenol, *m*-cresol, adenine) of optical density of 2.0 gave CD signals less than ±0.4 mdeg; and (3) the ratio of the CD amplitude of CSA at 290.5 nm to the sum of the absolute values of optical rotations at 275 and 306 nm was 0.773 (Cassim & Yang, 1969; Chen & Yang, 1977).[1] CD spectra, recorded in analog form on chart graphs, were digitized with a method based on image-processing techniques. Some spectra were also recorded on an AVIV 60DS spectorpolarimeter (Dept. of Chem., N.Y.U.) that met all three criteria.

RESULTS

Nucleotides per Protein Subunit. Spectra of Pf1 samples disrupted in *cracking buffer* are fit almost exactly with separate spectra for purified DNA and for purified protein (data every 0.1 nm from 250 to 340 nm). In this solvent DNA and protein are dissociated and denatured, as a consequence of which light scattering for $\lambda > 320$ nm becomes negligible (OD cm^{-1} $< 10^{-4}$). We used simple least-square multiregression to obtain the fits. The goodness-of-fit depends on the shapes of the spectra, hence the purity of the individual components relative to the purified virus. For two measurements each on two highly purified virus samples, the observed spectrum and the synthesized spectrum were virtually indistinguishable (Figure 2), and the regression correlation coefficients were $R^2 = 0.9999$; the apparent n/s was 1.00 for all four measurements (±0.01).

The actual value of the mole ratio n/s derived from the fits depends on the extinction coefficients of the two components, and herein lie the principal uncertainties. Pf1 DNA in the *cracking buffer* has $\epsilon(P) = 7830 \pm 200$ M^{-1} cm^{-1} at $\lambda = 260$ nm. This is based on $\epsilon(P) = 7700 \pm 140$ M^{-1} cm^{-1} for Pf1 DNA at 259 nm in 0.15 M NaCl and 0.015 M sodium citrate, pH 7.0 (Wiseman & Day, 1977). The small increase in

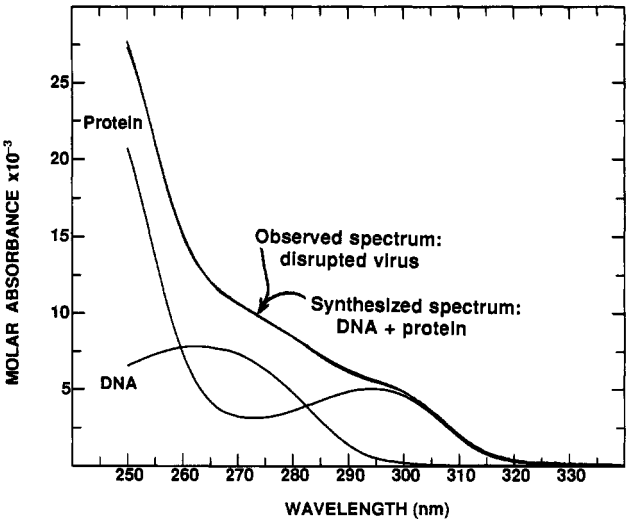

FIGURE 2: Molar absorbance spectrum of Pf1 virus disrupted in 0.2 M NaOH, 1% SDS, and 8 M urea, pH 13.3. The uppermost curve is actually the superposition of two spectra, the experimentally determined spectrum of disrupted virus and the best fit least squares spectrum based on the DNA and protein reference spectra.

uncertainty for the value in *cracking buffer* is due to random errors in pipeting. The coefficient reported by Wiseman and Day (1977) was the average of two values, 7763 and 7628, based on direct phosphorus determinations for two separate preparations; uncertainty cited being twice the difference between the values. A Pf1 protein extinction coefficient at $\lambda_{max} = 295$ nm for 0.5 M NaOH reported as 5070 ± 370 (Wiseman & Day, 1977) was the average of two values, 4934 and 5214. They were based on dry weight determinations for two preparations; here the cited uncertainty spans more than twice the difference. We found here that the value in *cracking buffer* is the same (±1%) as in 0.5 M NaOH. This protein value corresponds to a molar extinction coefficient of 2535 M^{-1} cm^{-1} per tyrosinate. Literature values for tyrosine itself under alkaline conditions (tyrosinate) are 2381 and 2406 M^{-1} cm^{-1} at 293.2 nm in 0.5 M NaOH [from Gratzer (1970) and Mihalyi (1970)], and we find 2500 M^{-1} cm^{-1} at 294 nm in *cracking buffer* and 2550 M^{-1} cm^{-1} at 295 nm in 95% EtOH and 0.5 M NaOH. The alkaline protein spectrum is red-shifted 2 nm and is 6% higher than the spectrum of two tyrosines in 0.5 M NaOH. From this set of numbers, we estimate a 6% uncertainty in n/s due to uncertainty in extinction coefficients. There is also systematic uncertainty on the order of 1% from the presence of minor proteins. Assuming five copies each of proteins encoded by open reading frames 30, 83, 437, and 141 in the virion as minor components (Hill *et al.*, 1991), we calculate a 1.3% contribution to the absorbance at 295 nm at pH 13.3. However, we assigned all protein absorbance to the major coat protein; n/s values would be systematically 1.3% too high if none of the minor protein interacts with the DNA. We estimate 7% overall uncertainty in our spectroscopic determination of n/s.

Two other virus preparations which had not been as highly purified gave n/s = 0.955 ± 0.015 ($R^2 = 0.9997$). A value of n/s = 0.92 was reported for virus samples disrupted in 0.5 M NaOH (Wiseman & Day, 1977). The same extinction coefficients were used in all studies. The lower n/s values correlate with lower A_{max}/A_{min} values and lower CD amplitudes (see below).

The value of n/s = 1.00 ± 0.07 from this analysis can be compared to a value of 1.05 ± 0.06 from measurements of

[1] Criteria 2 and 3 were satisfied for previously reported spectra from this laboratory and from a collaborating laboratory (Day, 1973; Day & Wiseman, 1978; Casadevall & Day, 1982; Cascadevall & Day, 1983; Day *et al.*, 1988a; Arnold *et al.*, 1992). This was not properly stated in the earlier papers.

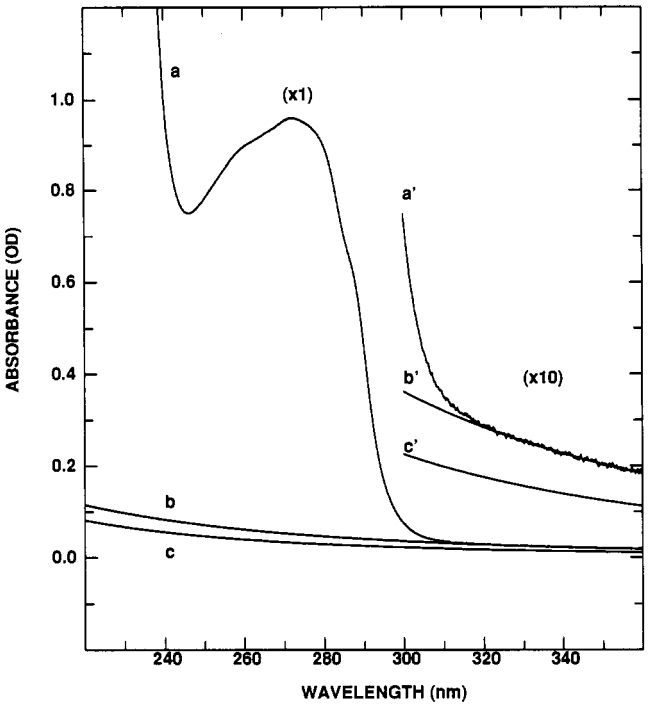

FIGURE 3: (a, a′) Absorbance and light scattering of intact Pf1 virus at 0.444 mg cm^{-3} in 1-cm pathlength cell in 10 mM sodium phosphate, pH 7.2 at room temperature; (b, b′) light scattering derived from optical density scans from 320–550 nm on this sample and extrapolation of the log τ vs log λ plot to lower wavelengths; (c, c′) theoretical light scattering calculated for a solution of rigid rods 2000 nm long with the molecular weight of Pf1.

total virion mass by STEM (Reisberg, 1989; Kostrikis *et al.*, 1991; Kostrikis, 1993) and values of 1.01 ± 0.02 from measurements of grams phosphorus per gram virus and 0.97 ± 0.06 from measurements of moles phosphorus per mole nitrogen (Wiseman & Day, 1977). On the basis of the n/s results in this study and these three other independent values, we conclude that the ratio of nucleotides to protein subunits in Pf1 virus is unity.

Native Pf1 Virus Ultraviolet Spectrum: Light-Scattering Contributions. An optical density spectrum for Pf1 virus in 10 mM sodium phosphate, pH 7.2, from 360 nm to below 240 nm is shown in Figure 3. The spectrum has a maximum at 272.5 ± 0.3 nm and a minimum at 246.0 ± 0.3 nm with an $A_{\lambda_{max}}/A_{\lambda_{min}}$ ratio = 1.28 ± 0.01 (without light-scattering correction). At lower wavelengths, there is a shoulder at 225 nm and a maximum at 190 nm (not shown). The light-scattering contributions to the optical density are relatively low for Pf1, even though its molecular weight is approximately 3.6×10^7. This is because intraparticle interference greatly reduces light scattering from a long rod as compared to scattering from a sphere of the same mass and volume (Neugebauer, 1943; van de Hulst, 1957; Geiduschek & Holtzer, 1958). (Interparticle interference can reduce the scattering further, and aggregation can increase it; the relative levels are affected by external conditions such as concentration and ionic strength.) For transmittance measurements, the intraparticle interference is parameterized by $Q(\lambda)$, a pure number between 0 and 1; the greater the intraparticle interference, the smaller the particle dissipation factor, $Q(\lambda)$. Nominal values of $Q(\lambda)$ for a rigid rod 2000 nm long are 0.064 at 320 nm, and 0.083 at 420 nm, whereas $Q(\lambda)$ values for a sphere of the same volume at these wavelengths are 0.48 and 0.68, respectively (Camerini-Otero & Day, 1978). This means that scattering from Pf1 is expected to be only about $^1/_8$ that from the equivalent sphere of the same mass. The turbidity relation is $\tau = H(\lambda)cM_rQ(\lambda)$; here $\tau = 2.303 \times$ OD cm^{-1}, c is concentration in g/cm^3, and $H(\lambda) = 32\pi^3 n(\lambda)^2 (dn(\lambda)/dc)^2/3N_A\lambda^4$ (Doty & Steiner, 1950). As is widely done, the scattering can be characterized by the slope of a plot of log τ vs log λ, which subsumes the wavelength dependencies of $H(\lambda)$ and $Q(\lambda)$ in a predictable way (Camerini-Otero & Day, 1978). Log (τ)–log (λ) plots for these samples of Pf1 from 320–550 nm had slopes of –3.86 in 10 mM sodium phosphate, pH 7.2; and –3.79 in 150 mM KCl, 10 mM sodium phosphate. A theoretical value is –3.82, calculated using dispersion parameters for H(λ) from Camerini-Otero and Day (1978) and a rigid-rod model for Pf1. The observed low scattering (Figure 3, curve b′) was found to be 50% higher than the calculated scattering (Figure 3, curve c′); flexing and/or low levels of lateral aggregation of the Pf1 filaments might account for this difference. For scattering in the region of absorbance, one must introduce a complex refractive index (van de Hulst, 1957). This did not seem necessary in this study because overall scattering is so low. We have estimated scattering in regions of absorbance from extrapolations of the log (τ) vs log (λ) plots into these regions. The spectrum shown in Figure 3 has light-scattering contributions of 5.4% at λ_{max} = 272.5 nm and 10.2% at λ_{min} = 246.0 nm (Figure 3, curve b). If anomalous scattering had been accounted for, the smooth curves b and c in Figure 3 would have had small oscillations which we estimate to be less than ±200 M^{-1} cm^{-1} in the 250–290-nm region, with minimal contributions directly at wavelengths of local absorbance maxima, and positive (negative) contributions above (below) it. This analysis is to show that scattering effects are small with respect to the absorbance assignments.

Native Pf1 Virus: Extinction Coefficients. The specific extinction coefficient and the molar extinction coefficient for intact Pf1 were obtained by diluting stock solutions into various measuring solutions, including the cracking buffer. For 0.15 M KCl and 0.010 M Na phosphate, pH 7.0, molar extinctions for intact Pf1 virus (per structure unit of one subunit and one nucleotide) after corrections for scattering are $\epsilon_{272.5nm}$ = 10400, ϵ_{259nm} = 9450, and ϵ_{246nm} = 7700. The specific coefficient for Pf1 virus at λ_{max} = 272.5 nm is 2.24 OD per mg/mL before light-scattering correction, and 2.12 OD per mg/mL after light-scattering correction. These values, which were used for all concentration determinations in the present study, are about 8% higher than corresponding values from virus dry weight measurements (Wiseman *et al.*, 1976).

Native Pf1 Virus: Absorbance by the Single-Stranded DNA and the Protein in the Virion. In Figure 4A we show absorbance spectra that have been assigned to the protein (two tyrosines) and to the DNA of Pf1 by means of a stepwise procedure. The procedure starts with the assignment of λ_{max} for the DNA in the virion. The free DNA has λ_{max} = 259 nm in neutral aqueous buffers and this does not change on melting. From the ready accessibility of the bases of Ag(I) and Hg(II) as probes (Casadevall & Day, 1982; Casadevall & Day, 1983; Day *et al.*, 1988b), one can conclude that the solvent around the bases is predominantly aqueous. Therefore we assign λ_{max} = 259 nm for Pf1 DNA *in situ*. Next we assign the average molar absorbance per nucleotide, ϵ(P), at this wavelength by subtracting an expected value for the absorbance of free isolated protein from the absorbance of the virus at this wavelength. The molar extinction coefficient per subunit (two tyrosines) is 1050 M^{-1} cm^{-1} in 1% SDS. To demonstrate that this is a suitable value to subtract from the virus absorbance, we show the spectra of tyrosine and its derivatives in five aqueous and nonaqueous solvents (Figure

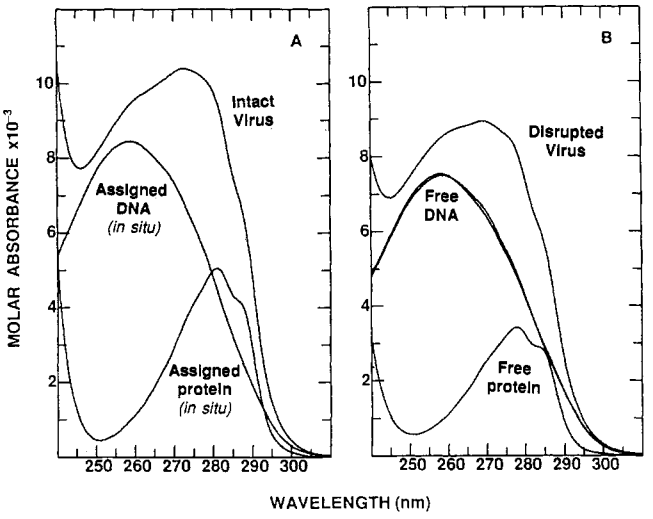

FIGURE 4: (A) Molar absorbance of intact Pf1 virus, with assigned *in situ* spectra for the single-stranded DNA and the coat protein. See text for method of construction of these *in situ* spectra. Part B is of alkali disrupted and then neutralized Pf1 virus in a final buffer of 0.2 M NaCl, 10 mM sodium phosphate, and 1% SDS. The protein spectrum is for pure protein dissolved in this buffer, corrected for light scattering. The label "Free DNA" is for two spectra: one is the neutral disrupted virus spectrum *minus* the protein spectrum, and the other is the spectrum for isolated DNA giving the best least-squares fit to the difference spectrum (R^2 = 0.9996).

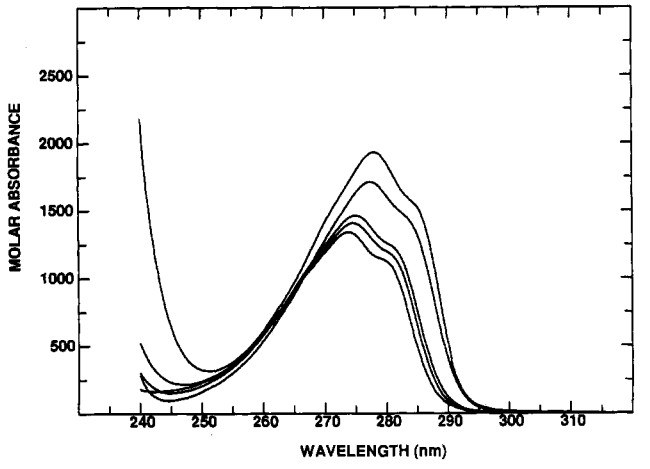

FIGURE 5: Molar absorbance spectra of tyrosyl chromophores in various solvents. Starting with the lowest spectrum $\epsilon_{\lambda max}$ at ~275 nm, the first four spectra are tyrosine in 90% 2,2,2-trifluoroethanol, in water, in 4% SDS, and in 90% ethanol. The highest spectrum is for AcTyrOEt in 100% ethanol.

5); although the specta show red-shifts and large changes in absorbance overall, in each solvent used the absorbance at 259 nm in the weak park of the near-UV tyrosine band is within 10% of an average of 527 M^{-1} cm^{-1} at 259, giving an average of 1054 M^{-1} cm1$-^{1}$ for two tyrosines. Thus we subtract the actual value of 1050 M^{-1} cm^{-1} for the protein in SDS from 9450 M^{-1} cm^{-1} to obtain 8400 M^{-1} cm^{-1} for the average nucleotide in the virion. If λ_{max} for the DNA *in situ* should be above or below 259 nm, this estimated ϵ(P) value would change little because both protein and virus spectra are increasing monotonically in this region. Having assigned ϵ-(P) at this one wavelength, we next assign the *in situ* DNA spectrum as the spectrum of heat denatured isolated Pf1 DNA at 80 °C. This spectrum, shown in Figure 4A, has λ_{max} = 259 nm and $\epsilon(P)_{259nm}$ = 8400 M^{-1} cm^{-1}; melting curves of Pf1 DNA show a gradual increase of $\epsilon(P)_{259nm}$ from 8350, at 70 °C, to 8400, at 80 °C, to a plateau of 8450 M^{-1} cm^{-1}, beginning at 90 °C (data not shown). Having assigned a DNA spectrum, we then assign the protein spectrum by subtracting the DNA spectrum from the virus spectrum (Figure 4A). This assigned protein spectrum looks like a red-shifted tyrosyl spectrum, and its numerically generated derivative spectrum has features characteristic of tyrosyl model compounds. On the basis of this, and other tests, we assign, for the average tyrosyl in the virion, an $\epsilon_{\lambda_{max}}$ = 2500 in the near UV, higher than for most, if not all, tyrosines, and λ_{max} = 281.5 nm. This assignment procedure is independent of whether or not there are any spectroscopic interactions between the bases and tyrosines.

Our assignments predict a drop in absorbance upon disruption of the virus under conditions that allow base–base stacking in the released single-stranded DNA and normal tyrosine absorbance in the released protein. This is precisely what is observed; when we neutralize solutions of Pf1 after alkaline disruption, we observe spectra that are reduced in amplitude at every wavelength, relative to the spectrum of native virus (Figure 4B). The final buffer for Figure 4B is 0.2 M NaCl, 10 mM Na phosphate, and 1% SDS, pH 7.0, in which $\epsilon(P)_{259nm}$ = 7500 for Pf1 DNA and $\epsilon_{277.5nm}$ = 3400 for the subunit. The reduction in absorbance at all wavelengths, on passage from conditions of Figure 4A to those of Figure 4B, confirms that bases and tyrosines absorb more in the virion than they do in the neutralized mixture.

Clack and Gray (1992) also observed that the tyrosyl absorbance is abnormally high and red-shifted, but they assigned spectra to DNA and protein with shapes different from those in FIgure 4A, and they assigned an ϵ(P) of only 6030 ± 390 M^{-1} cm^{-1} for *in situ* Pf1 DNA. Clack and Gray (1992) used a value for ϵ(P) of free Pf1 DNA at 80 °C that we believe is too high, and they did not allow for differences in shapes of tyrosyl spectra in the fitting procedure they used in assigning the Pf1 virus absorbance spectrum.

Support of the strong red-shift for tyrosine (Figure 4A) comes from comparisons of the absorbance and CD spectra for virus with absorbance and CD spectra of tyrosine and the free protein (Figure 6). The positive CD spectrum of the free amino acid L-Tyr is weak. The negative CD spectrum for isolated protein is stronger and shifted to the red. The negative CD of the intact virion is stronger still, and even more red-shifted. The absorbance spectra show similar trends. For all three pairs of CD and absorbance spectra, the λ_{max} and the $\lambda_{shoulder}$ of the features correspond within ±0.3 nm. Part of the negative CD above 250 nm of the intact virion can be reversibly titrated, with a pK_a of 11.4 (data not shown), which is the pK_a as assigned to Y_{25} from absorbance and fluorescence titrations. The correspondence in shape and λ_{max} of this CD and the absorbance assigned to tyrosine in the virion leads us to assign this CD largely to tyrosine Y_{25}. Also, it is seen that the assigned *in situ* absorbance of protein dips slightly below the absorbance of isolated protein near 250 nm (Figure 6). This effect is on the order of variations in literature values for this minimum, and it is also on the order of expected anomalous light-scattering contributions to the assigned absorbance. Anomalous scattering contributes positively to the assigned tyrosine absorbance near 281.5 nm and negatively near 250 nm.

CD of Pf1 from 250 to 310 nm Shows No Evidence of Base–Base Stacking. In Figure 7 we compare measured CD spectra of intact Pf1 virus, of isolated protein (expressed per mole of nucleotide), and of isolated Pf1 DNA, and a calculated CD spectrum for a mixture of free nucleoside monophosphates. The spectrum of *isolated* single-stranded Pf1 DNA looks like the well-known bimodal, "conservative" spectrum of B-form

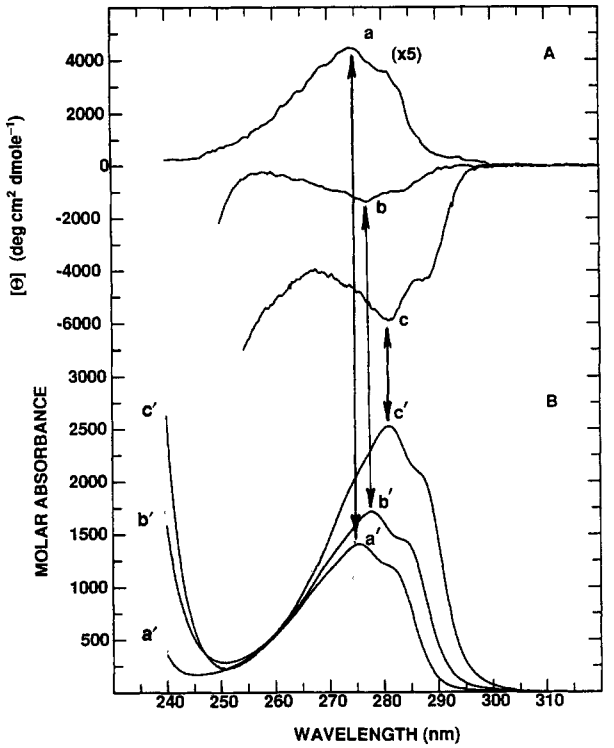

FIGURE 6: Circular dichroism (A) and ultraviolet absorbance (B) of (a, a′) L-Tyr, (b, b′) isolated protein, and (c, c′) purified Pf1 virus. The CD and UV are presented as molar ellipticities and molar absorbancies per tyrosine. L-Tyr and isolated protein were in 10 mM sodium phosphate and 1% SDS, pH 7.2, and Pf1 virus was in 10 mM sodium phosphate pH 7.2. The correctness of the derived *in situ* protein absorbance spectrum c′ is supported by the fact that its characteristic features (λ_{max}, $\lambda_{shoulder}$, and shape) correspond with these features of its CD, in the same manner that these features of free tyrosine and isolated protein absorbance and CD spectra correspond to each other.

DNA, the result of the base–base stacking interactions that give rise to DNA CD (Warshaw *et al.*, 1965; Tinoco *et al.*, 1980; Johnson *et al.*, 1981). Extensive stacking in the isolated single-stranded DNA (base composition 19.4% A, 19.1% T, 31.3% C, 30.2% G) is expected; stacking interactions in single-stranded nucleic acids are well known, and it is reflected in the extinction coefficient in this buffer of $\epsilon(P) = 7400$. The calculated free nucleotide spectrum is weaker and has a different shape; it stems from chiralities induced in the base chromophores by the sugars, not from stacking. The CD of intact Pf1 virus neither looks like that of the isolated Pf1 DNA nor that of the nucleotide mixture; as just discussed above, it has very nearly the shape of the absorbance spectrum assigned to the two *in situ* tyrosines, but much of the CD band is characterized by a p*K* of only one of them. Preliminary attempts to assign the near-UV CD have been done by subtracting the portion which appears to belong to Y_{25}; this leaves a spectrum of low negative amplitudes from 280 nm down to 250 nm assignable jointly to an average nucleotide and Y_{40}. It does not look like literature spectra for base-stacked DNA in any of its known conformations (Pohl & Jovin, 1972; Sprecher & Johnson, 1977; Sprecher *et al.*, 1979; Johnson *et al.*, 1981; Bokma *et al.*, 1987). There is no suggestion of an underlying CD contribution from any of A–, B–, or Z-form DNA, and in fact, it looks as if no DNA were present, even though DNA dominates the near-UV absorbance. We find no evidence for base–base stacking in the CD spectrum of intact Pf1. This is consistent with the high $\epsilon(P)$ assigned to the DNA absorbance.

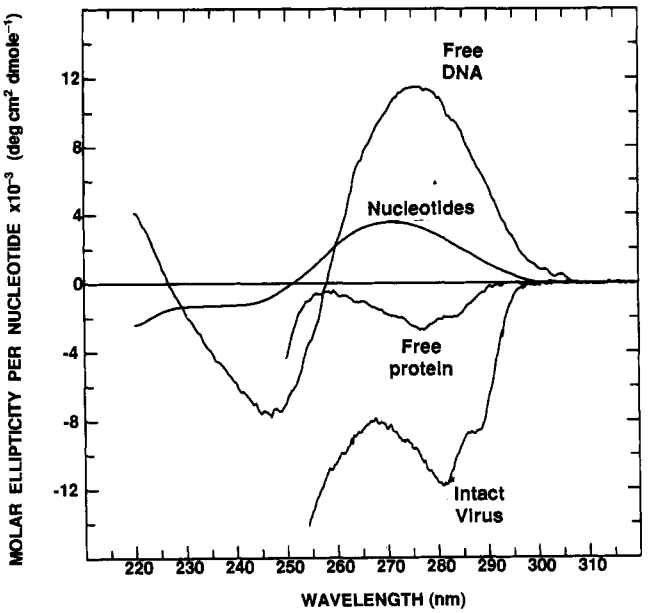

FIGURE 7: Circular dichroism spectra of purified Pf1 virus, isolated DNA and protein, and the weighted sum of the constituent nucleotides (Sprecher & Johnson, 1977). The CD amplitudes are molar ellipticities per average nucleotide. The concentrations for the purified virus and the isolated protein were based on extinction coefficients of 2.12 mg^{-1} cm^2 at 272.5 nm for Pf1 virus (see text) and 0.37 mg^{-1} cm^2 at 277.5 nm for the isolated Pf1 protein (see text). Both extinction coefficients are for samples after light-scattering corrections.

Further Analyses of Tyrosines in the Virion. As the solvent becomes less polar, the spectrum for the tyrosyl chromophore becomes red-shifted and the molar extinction coefficient increases (Figure 5). Brandts and Kaplan (1973) characterized the shapes of such spectra in terms of derivative spectra, finding that they correlated with the H-bonding properties of the solvents. The shapes of derivative spectra of L-Tyr and AcTyrOEt in solvents which can both accept and donate protons are distinct from those of the spectrum of AcTyrOEt in ethyl acetate, a solvent that has no protons available for H-bonds (Brandts & Kaplan, 1973). Derivative spectra (data not shown) were generated for protein in the virus (Figure 4A), for isolated protein (Figure 4B), and each of the spectra in Figure 5. The two protein derivative spectra obtianed look like those for tyrosyl in nonpolar solvents which are both acceptors and donors of hydrogen bonds, not like those in ethyl acetate (Kostrikis, 1993). Thus, on the basis of their absorbance properties, both tyrosines appear to be H-bond acceptors and H-bond donors, and their solvent environments appear to be nonpolar.

Circular Dichroism of Native Pf1 from 185 to 250 nm. CD spectra in the wavelength region where protein backbone contributions dominate are given in Figure 8. The CD of the intact Pf1 virus has a positive band at 190 nm and two negative bands at 207.5 and 221 nm with magnitudes of $[\theta]_{190nm}$ = +95 000, $[\theta]_{207.5nm}$ = −44 000, and $[\theta]_{221nm}$ = −40 000 deg cm^2 $dmol^{-1}$. The crossover from negative to positive ellipticity occurs at 199.7 nm. The uncertainties in the amplitudes are on the order of ±5%, due to uncertainty in concentration. These amplitudes are higher than previously reported values for Pf1 virus (Day & Wiseman, 1978; Casadevall & Day, 1982; Day *et al.*, 1988a; Clack & Gray, 1989), the increases being more than the 8% increase called for by the increase in virus extinction coefficient. Our less pure virus samples have had lower CD amplitudes at all wavelengths.

The CD of isolated protein in 1% SDS (Figure 8) was found to have $[\theta]_{190nm}$ = +51 000, $[\theta]_{208nm}$ = −28 000, and $[\theta]_{222nm}$

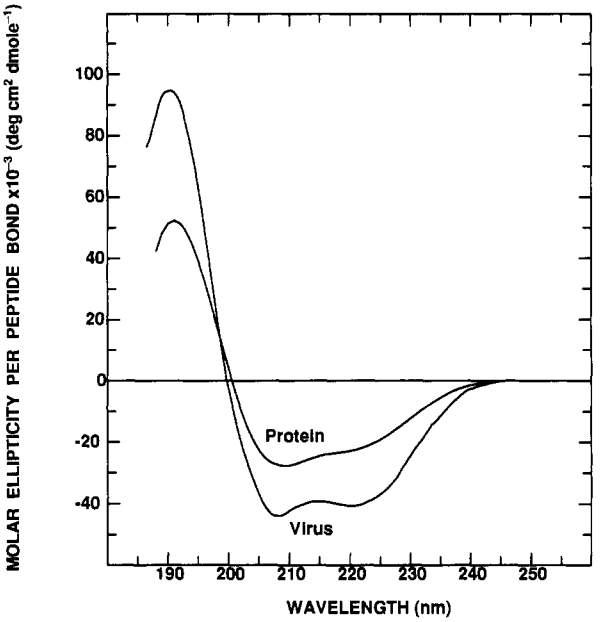

FIGURE 8: Circular dichroism spectra for purified Pf1 virus and isolated Pf1 protein.

= −23 000 deg cm^2 dmol^{-1}. A CD spectrum of Pf1 virus that had been alkali denatured and neutralized (spectrum not shown) was virtually identical in shape to the spectrum of the isolated protein, even though these solutions contain DNA whereas the former solutions do not; the neutralized mixture gave $[\theta]_{190nm}$ = +56 000, $[\theta]_{208nm}$ = −31 000, and $[\theta]_{222nm}$ = −25 000 deg cm^2 dmol^{-1}. The ~10% amplitude differences between the mixtures containing DNA and the solutions of pure protein are not due directly to the free DNA present because free DNA contributions are much weaker (barely distinguishable from baseline in Figure 8) and differ in shape. These spectra for protein in the neutral buffer containing SDS, both with and without DNA, have the crossover from negative to positive ellipticity at 200.5 nm instead of at 199.7 nm.

It is unlikely that differential CD scattering (Tinoco *et al.*, 1980) would affect the CD of this particular virus in any significant way. This is because the diameter of the virus is very small relative to the wavelength, there are no long wavelength tails, and such spectra have negligible corrections for Duysen flattening (Day & Hoppensteadt, 1972).

DISCUSSION

The Stoichiometric Ratio of Unity and Implications for Pf1 DNA Structure. Previous attempts to obtain n/s spectroscopically gave variable results, and in this study we observed variability in n/s, lower values correlating with lower CD amplitudes and usually with virus preparations of lesser purity. Obtaining reliable results with this method on the highest purity samples in the current series gives us confidence both in the unit ratio obtained and in the correctness of the spectroscopic properties of these preparations.

The unit n/s ratio in Pf1 is unique among filamentous viruses, and to our knowledge, unique among all nucleoproteins. The unit ratio pertains to nucleotides and major coat protein subunits all along the length of the virion. A few nucleotides at the ends of the Pf1 virion, expected to be fewer than 1% of the 7349 residues in the entire sequence, are involved in the fold-back regions, presumably having specific interactions with minor protein subunits (Russel & Model, 1989; Hill *et al.*, 1991). The unit ratio means, therefore, that there are approximately 7300 nucleotides and 7300 subunits along the contour. A helical structure is described by the axial rise and rotation of its structure elements. Since there are two oppositely directed DNA strands, the axial separation per nucleotide along each DNA strand must be twice that of the axial rise per subunit in the protein helix. The protein subunit helix is a simple one-start helix with an axial rise per subunit in the range 2.90 to 3.05 Å and a rotation per subunit in the range 65.9° to 66.7°, depending on the state of chemical modification and/or external conditions (Nave *et al.*, 1981). Therefore the axial rise per nucleotide is in the range 5.8 to 6.1 Å, the longest known for any two-stranded nucleic acid. We think it interesting and significant that the structure holding the DNA in the conformation with the longest rise per residue is also the structure with the unique unit nucleotide/subunit ratio.

The nucleotide axial rise of Pf1 DNA is an established fact, but the rotation per nucleotide residue is not. Our interpretation of the unit ratio is that it implies a DNA helix with the same pitch as the protein helix, so that successive nucleotides in one strand of the DNA helix interact with every other subunit in the protein helix. Thus, for each DNA strand, the rotation per nucleotide becomes twice the rotation per protein subunit in the protein helix. This is the simplest interpretation, and the interpretation giving the most symmetrical structure, but it couples the extreme rise per nucleotide of about 6 Å with an unprecedented rotation per nucleotide lying in the range 131.8° to 133.4°. Since all the subunits are oriented the same way with respect to the virus axis ("up"), but the strands of DNA in the center are antiparallel, the unit interaction idea calls for two types of nucleotide–subunit interactions, "up" and "down", so that the stoichiometric ratio can be written as n/s = 2/2.

Pf1 DNA Structure Models and the Observed Spectral Features. In each strand, the axial rise of ~6 Å and a rotation of ~133° makes the distance between bases too great for base–base stacking, and steric hindrance between the sugar-phosphate backbones prevents simple stacking between bases in opposite strands [see Day *et al.* (1979, 1988a)]. Therefore we find it completely understandable that the DNA part of the UV absorbance spectrum of Pf1 can be assigned as the spectrum for heat denatured DNA, and that the CD spectrum shows no evidence, whatsoever, for base–base stacking. The enormous values for the axial rise and the rotation per nucleotide in this type of DNA helix model forces the phosphates to the center; the radial positions of phosphorus atoms of the backbone are at radii of maximally about 2.5 Å (Day *et al.*, 1979; Marzec & Day, 1983; Day *et al.*, 1988a). In the absence of an acceptable detailed model of this part of Pf1 structure, it is difficult to visualize how this DNA is held by the protein, such as how the phosphate charges are neutralized by the lysyl and/or argininyl groups of the protein subunits, or how the two DNA strands are placed relative to each other and to the protein helix. To provide at least the fundamental symmetry relations proposed and some sense of the 3-D relations involved, we present in Figure 9 a schematic diagram of the three helices, the helix of subunits, the "up" strand of DNA, and the "down" strand of DNA. The relative axial and azimuthal displacements of the two DNA strands represented in Figure 9 were set to maximize inter-phosphate distances.

A number of other spectroscopic studies place constraints on Pf1 DNA structure, and satisfactory models must accommodate such data. ^{31}P NMR studies or oriented Pf1 show that the DNA in Pf1 is ordered such that there is perhaps only

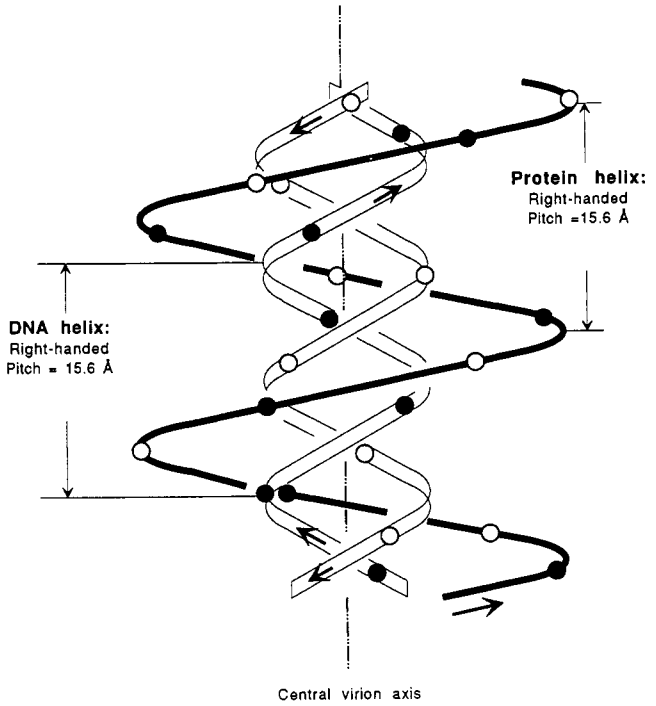

FIGURE 9: A diagram of the interpretation of the unit stoichiometric ratio in terms of equal pitches for the helix of protein subunits, traced by the solid line, and the "up" and "down" strands of DNA, represented by the interwoud ribbons at the center which define, approximately, the radial boundary at 6 Å between the bases outside and the sugar–phosphate backbones inside. The helices are right-handed in this diagram, and the pitches are 16 Å. Although detailed models of this part of Pf1 structure are not yet available, the stereochemical feasibility of DNA with such a low pitch and high axial rise has been shown (Day *et al.*, 1979, 1988a). The black and white dots along the outer solid helix, arbitrarily placed at about 16-Å radius in this diagram, represent the position of each subunit in the protein helix; the subunits are all oriented in one way, "up" for example, but the positions of some atoms in each subunit must vary to accommodate the base type and whether the nucleotide is in the "up" (black) or "down" (white) strand. The region between the outer solid line and the ribbons contains protein contributions from C-terminal amino acids and the bases. The large base-to-base distance explains why the bases in such a DNA can have the high UV absorbance of heat denatured DNA and no recognizable near-UV CD.

one environment for the phosphate group (Cross *et al.*, 1983). Raman studies show that the nucleoside sugar pucker and glycosyl torsion of the DNA in Pf1 is C2′-endo/anti (Thomas *et al.*, 1988). Linear dichroism data on flow-oriented samples (Clack & Gray, 1992) and birefringence measurements on magnetically oriented samples (Torbet & Maret, 1981) both indicate substantial tilts of the planes of the bases, so they are not perpendicular to the structure axis. A Pf1 DNA model proposed recently by Marvin *et al.* (1992) contradicts these spectroscopic data and has six different nucleotide–subunit environments; because it is in conflict with so much data, we consider that model to be incorrect. DNA models which do satisfy the constraints of the data (Day *et al.*, 1979; Marzec & Day, 1983; Day *et al.*, 1988a), have been based on the idea that, in this particular filamentous bacteriophage, the pitch of the DNA helix and the pitch of the protein helix are the same.

Base–Tyrosine Interactions in Pf1. We have accounted for the CD and absorbance spectra in terms of separate contributions from DNA bases and from tyrosines. This does not mean, however, that direct base–tyrosine interactions do not occur. All of the Y_{40} residues may be close enough to bases to completely quench their fluorescence (Day *et al.*, 1979; Greulich & Wijnaendts Van Resandt, 1984). The derivative absorbance analysis indicates that tyrosines are H-bond donors and H-bond acceptors (Kostrikis, 1993), as found by Raman spectroscopy (Thomas *et al.*, 1983). Base–tyrosyl hydrogen bonding could occur at Y_{40}. Direct base–tyrosine interactions may account for some, or all, of the subtle effects of temperature on Pf1 CD (Casadevall & Day, 1988).

The Conformation of the Protein Subunit and the Case for 3_{10}-Helices. The dominant feature of the CD is the α-helix contribution. It has been accepted for a long time that the protein in the Pf1 virion is highly α-helical (Marvin *et al.*, 1974; Thomas & Murphy, 1975; Day & Wiseman, 1978), but the exact fraction of the 46 residues in the α-helical range of conformation is difficult to establish. The Raman spectra show almost perfect α-helical character (Thomas & Murphy, 1975; Thomas *et al.*, 1983; Thomas & Agard, 1984), and the CD amplitudes for the intact virion from 185 to 250 nm (Figure 8) are among the highest recorded for helical polypeptides or proteins. Because the amplitudes are higher than many reference amplitudes for pure α-helix, CD analysis programs have not been used in this study. In addition, the CD analysis programs do not yet include contributions from 3_{10}-helices.

There appear to be contributions from 3_{10}-helix to the Pf1 far UV CD spectrum. The two relevant facts are (a) the CD amplitudes are as high or higher than nominal values for all reference spectra for pure α-helices, even for polypeptides (Holzwarth *et al.*, 1962; Holzwarth & Doty, 1965; Carver *et al.*, 1966; Greenfield & Fasman, 1969; Chen *et al.*, 1974; Chen & Yang, 1977; Brahms & Brahms, 1980; Johnson, 1988; Sreerama & Woody, 1993) and (b) available experimental and theoretical spectra for 3_{10}-helices, while similar in shape to α-helix spectra, are blue-shifted 5–8 nm, tend to have stronger 208-nm bands than 222-nm bands, and have, in some cases, higher amplitudes (Manning & Woody, 1991; Miick *et al.*, 1992). We think that the crossover for Pf1 virus at 199.7 nm, the greater amplitude at 207.5 nm than at 221 nm, and the high amplitudes overall, all combine to hint that there is 3_{10}-helix in Pf1 virus. The hint is strengthened in that four other filamentous viruses, with structures similar to that of Pf1 in their most general aspect, have amplitudes at 222–223 nm greater than amplitudes at 208 nm, and the crossovers from negative to positive ellipticity that range from 201 to 203 nm (Day *et al.*, 1988; Clack & Gray, 1989; Arnold *et al.*, 1992). Further, the isolated Pf1 protein in the SDS detergent solution (Figure 8) has lower amplitudes and a longer wavelength crossover, indicating a difference in the secondary structure of the protein in the virus and in this detergent solution; the difference may include the presence of 3_{10}-helix in the virion but not in the free protein.

The presence of one or a few turns of 3_{10}-helix may resolve some of the current problems in establishing a viable model for Pf1 virus structure. It would be difficult to reconcile the present CD data with a subunit conformation that is anything but perfectly helical, either all α-helix, or mostly α-helix with some 3_{10}-helix. Therefore the seven residue nonhelical loop between two "idealized" α-helical segments totaling 39 residues for the subunit proposed by Nambudripad *et al.* (1991a,b) appears to be in direct conflict with our data. The local helix phasing possibilities allowed by 3_{10}-helices and α-helices in their ranges of torsion angles (Barlow & Thornton, 1988) might provide sufficient modeling lattitude to accomodate constraints provided by the neutron diffraction data (Nambudripad *et al.*, 1991a). Our protein CD data can be more easily reconciled with the protein models of the type proposed by Marvin *et al.* (1987) or of the type proposed by Marzec and Day (1988). Although some modeling of the Pf1 subunit

has included 3_{10}-helices (unpublished work of M. Bansal, E. J. Wachtel, and D. A. Marvin cited by Marvin, 1985), the three current published approaches to Pf1 protein models (Marvin *et al.*, 1987; Marzec & Day, 1988; Nambudripad *et al.*, 1991a) have α-helix as the only recognized structure motif.

Further with respect to the protein structure, if our interpretation of the unit stoichiometry is correct, then any analysis of the diffraction data must be based on an asymmetric unit containing two protein subunits and two nucleotides. However, published analyses to date have used one protein subunit without a nucleotide as the asymmetric unit, and it has been accepted for sometime that the structural repeat of Pf1 in fibers at temperatures near 20 °C has 27 protein subunits in five turns over about 75 Å (Marvin *et al.*, 1974; Wiseman & Day, 1977; Makowski & Caspar, 1981). The relation n/s = 2/2 requires even numbers of nucleotides and subunits in the repeat, opening the possibility that the correct number might be 26 or 28. If 27 is the correct number, then the "true repeat" would contain 27 pairs of subunits and 54 nucleotides in 10 turns over 150 Å.

CONCLUSION

The present data are consistent only with DNA models having no base–base stacking interactions. The data are consistent with protein subunit models having as many as two or three turns of 3_{10}-helix in an otherwise α-helical protein subunit. In our view, the key to correct virion structure models lies in the DNA structure and its relation to the surrounding helix of protein.

ACKNOWLEDGMENT

We thank Y. K. Yip (P.H.R.I.) for help with the protein sequencing, C. J. Marzec and R. E. Hendrix (P.H.R.I.) for discussions, and D. Rentzeperis and L. A. Marky (N.Y.U.) for making instruments for some of the measurements available to us.

REFERENCES

Arnold, G. E., Day, L. A., & Dunker, A. K. (1992) *Biochemistry 31*, 7948–7956.
Barlow, D. J., & Thornton, J. M. (1988) *J. Mol. Biol. 201*, 601–619.
Bokma, J. T., Johnson, W. C., & Blok, J. (1987) *Biopolymers 26*, 893–909.
Bradley, D. E. (1973) *Can. J. Microbiol. 19*, 623–632.
Brahms, S., & Brahms, J. (1980) *J. Mol. Biol. 138*, 149–178.
Brandts, J. F., & Kaplan, L. J. (1973) *Biochemistry 12 (10)*, 2011–2024.
Camerini-Otero, R. D., & Day, L. A. (1978) *Biopolymers 17*, 2241–2249.
Carver, J. P., Schechter, E., & Blout, E. R. (1966) *J. Am. Chem. Soc. 88*, 2550–2561.
Casadevall, A., & Day, L. A. (1982) *Nucleic Acids Res. 10*, 2467–2481.
Casadevall, A., & Day, L. A. (1983) *Biochemistry 22*, 4831–4842.
Casadevall, A., & Day, L. A. (1988) *Biochemistry 27*, 3599–3602.
Cassim, J. Y., & Yang, J. T. (1969) *Biochemistry 8*, 1947–1951.
Chen, G. C., & Yang, J. T. (1977) *Anal. Lett. 10 (14)*, 1195–1207.
Chen, Y., Yang, J. T., & Chau, K. H. (1974) *Biochemistry 13*, 3350–3359.
Clack, B. A., & Gray, D. M. (1989) *Biopolymers 28*, 1861–1873.
Clack, B. A., & Gray, D. M. (1992) *Biopolymers 32*, 795–810.
Cross, T. A., Tsang, P., & Opella, S. J. (1983) *Biochemistry 22*, 721–726.
Day, L. A. (1973) *Biochemistry 12*, 5329–5339.
Day, L. A., & Hoppensteadt, F. (1972) *Biopolymers 11*, 2131–2140.
Day, L. A., & Wiseman, R. L. (1978) in *The Single-Stranded DNA Phages* (Denhardt, D. T., Dressler, D., & Ray, D. S., Eds.) pp 605–625, Cold Spring Harbor Lab., New York.
Day, L. A., Wiseman, R. L., & Marzec, C. J. (1979) *Nucleic Acids Res. 7*, 1393–1403.
Day, L. A., Marzec, C. J., Reisberg, S. A., & Casadevall, A. (1988a) *Ann. Rev. Biophys. Biophys. Chem. 17*, 509–539.
Day, L. A., Casadevall, A., Prescott, B., & Thomas, G. J. (1988b) *Biochemistry 27*, 706–711.
Doty, P., & Steiner, R. F. (1950) *J. Chem. Phys. 18*, 1211–1220.
Geiduschek, E. P., & Holtzer, A. (1958) *Adv. Biol. Med. Phys. 6*, 431
Gratzer, W. (1970) in *CRC Handbook of Biochemistry* (Sober, H. A., Ed.) 2nd ed., B74, CRC, Cleveland.
Greenfield, N. J., & Fasmann, G. D. (1969) *Biochemistry 8*, 4108–4116.
Greulich, K. O., & Wijnaendts Van Resandt, R. (1984) *Biochim. Biophys. Acta 782*, 440–449.
Hill, D. F., Short, N. J., Perham, R. N., & Petersen, G. B. (1991) *J. Mol. Biol. 218*, 349–364.
Holzwarth, G., & Doty, P. (1965) *J. Am. Chem. Soc. 87*, 218–228.
Holzwarth, G., Gratzer, W. B., & Doty, P. (1962) *J. Am. Chem. Soc. 84*, 3194–3196.
Johnson, W. C., Jr. (1988) *Ann. Rev. Biophys. Biophys. Chem. 17*, 145–166.
Johnson, B. B., Dahl, K. S., Tinoco, I., Ivanov, V. I., & Zhurkin, V. B. (1981) *Biochemistry 20*, 73–78.
Knippers, R., & Hoffmann-Berling, H. (1966) *J. Mol. Biol. 21*, 305–312.
Kostrikis, L. G. (1993) Architectural studies on filamentous bacterial viruses: Pf1, Epf1, and C2, Ph.D. Thesis, New York University.
Kostrikis, L. G., Reisberg, S. A., Simon, M. N., Wall, J. S., & Day, L. A. (1991) *Mol. Microbiol. 5*, 2641–2647.
Makowski, L., & Caspar, D. L. D. (1978) in *The Single-Stranded DNA Phages* (Denhardt, D. T., Dressler, D., & Ray, D. S., Eds.) pp 627–643, Cold Spring Harbor Laboratory, New York.
Makowski, L., & Caspar, D. L. D. (1981) *J. Mol. Biol. 145*, 611–617.
Manning, M. C., & Woody, R. W. (1991) *Biopolymers 31*, 569–586.
Marvin, D. A., Wiseman, R. L., & Wachtel, E. (1974), *J. Mol. Biol. 82*, 121–138.
Marvin, D. A., Bryan, R. K., & Nave, C. (1987) *J. Mol. Biol. 193*, 315–343.
Marvin, D. A., Nave, C., Bansal, M., Hale, R. D., & Salje, E. K. (1992) *Phase Transitions 39*, 45–80.
Marzec, C. J., & Day, L. A. (1983) *Biophys. J. 42*, 171–180.
Marzec, C. J., & Day, L. A. (1988) *Biophys. J. 53*, 425–440.
Mihalyi, E. (1970) in *CRC Handbook of Biochemistry* (Sober, H. A., Ed.) 2nd ed., pp B75–77, CRC, Cleveland.
Miick, S. M., Martinez, G. V., Fiori, W. R., Todd, A. P., & Millhauser, G. L. (1992) *Nature 359*, 653–655.
Nambudripad, R., Stark, W., & Makowski, L. (1991a) *J. Mol. Biol. 230*, 359–379.
Nambudripad, R., Stark, W., Opella, S. J., & Makowski, L. (1991b) *Science 252*, 1305–1308.
Nave, C., Fowler, A. G., Ladner, J. E., Marvin, D. A., Provencher, S. W., Tsugita, A., Armstrong, J., & Perham, R. N. (1981) *J. Mol. Biol. 149*, 675–707.
Neugebauer, T. (1943) *Ann. Phys. 42*, 509.
Pohl, F., & Jovin, T. (1972) *J. Mol. Biol. 67*, 375–396.
Reisberg, S. A. (1989) Radial mass density profiles, mass per length, and nucleotide/subunit ratios for filamentous bacte-

riophages from electron microscopy, PhD Thesis., New York University.
Russel, M., & Model, P. (1989) *J. Virol. 63*, 3284–3295.
Sprecher, C. A., & Johnson, W. C., Jr. (1977) *Biopolymers 16*, 2243–2264.
Sprecher, C. A., Baase, W. A., & Johnson, W. C. (1979) *Biopolymers 18*, 1009–1019.
Sreerama, N., & Woody, R. W. (1993) *Anal. Biochem. 209*, 32–44.
Takeya, K., & Amako, K. (1966) *Virology 28*, 163–165.
Thomas, G. J., Jr., & Murphy, P. (1975) *Science 188*, 1205–07.
Thomas, G. J., Jr., & Agard, D. A. (1984) *Biophys. J. 46*, 763–768.
Thomas, G. J., Jr., Prescott, B., & Day, L. A. (1983) *J. Mol. Biol. 165*, 321–356.
Thomas, G. J., Jr., Prescott, A. B., Opella, S. J., & Day, L. A. (1988) *Biochemistry 27*, 4350–4357.
Tinoco, I., Jr., Bustamante, C., & Maestre, M. F. (1980) *Ann. Rev. Biophys. Bioeng. 9*, 107–141.
Torbet, J., & Maret, G. (1981) *Biopolymers 20*, 2657–2669.
van de Hulst, H. C. (1957) *Light Scattering by Small Particles*, John Wiley and Sons, New York.
Warshaw, M. W., Bush, C. A., & Tinoco, I. (1965) *Biochem. Biophys. Res. Commun. 18*, 633–638.
Wiseman, R. L., & Day, L. A. (1977) *J. Mol. Biol. 116*, 607–611.
Wiseman, R. L., Berkowitz, S. A., & Day, L. A. (1976) *J. Mol. Biol. 102*, 549–561.
Yamamoto, K. R., Alberts, B. M., Benzinger, R., & Lawhorne, L. (1970) *Virology 40*, 734–744.